

# **Geophysical Research Letters**\*

#### RESEARCH LETTER

10.1029/2025GL118583

#### **Key Points:**

- · Suppressing sub-synoptic soil moisture (SM) heterogeneity (<1,000 km) decreases peak Mesoscale Convective System (MCS) population by 23%, without weakening convective intensity
- Mesoscale dry soil patches (100-500 km) modify the Sahelian boundary layer such that conditions are more favorable for mature MCS passage
- · Increased insolation in cloud-free slots can replace dry SM as a source of favorable MCS conditions, in tandem with background monsoon flow

#### **Supporting Information:**

Supporting Information may be found in the online version of this article.

#### Correspondence to:

B. Maybee, b.w.maybee@leeds.ac.uk

Maybee, B., Klein, C., Taylor, C. M., Burns, H., & Marsham, J. H. (2025). Homogeneous soil moisture fields suppress Sahelian MCS frequency. Geophysical Research Letters, 52, e2025GL118583. https://doi.org/10.1029/ 2025GL118583

Received 4 AUG 2025 Accepted 7 NOV 2025

#### **Author Contributions:**

Conceptualization: Ben Maybee. Cornelia Klein, Christopher M. Taylor, John H. Marsham

Data curation: Helen Burns Formal analysis: Ben Maybee, Cornelia Klein

Funding acquisition: Cornelia Klein, Christopher M. Taylor, John H. Marsham Investigation: Ben Maybee,

Cornelia Klein

Methodology: Ben Maybee, Cornelia Klein, Christopher M. Taylor, John H. Marsham

Project administration: Cornelia Klein Software: Ben Maybee, Helen Burns

© 2025. The Author(s). This is an open access article under the terms of the Creative Commons Attribution License, which permits use, distribution and reproduction in any medium, provided the original work is properly cited.

## Homogeneous Soil Moisture Fields Suppress Sahelian MCS **Frequency**

Ben Maybee<sup>1</sup>, Cornelia Klein<sup>2</sup>, Christopher M. Taylor<sup>2,3</sup>, Helen Burns<sup>1</sup>, and John H. Marsham<sup>1</sup>

<sup>1</sup>School of Earth and Environment, University of Leeds, Leeds, UK, <sup>2</sup>UK Centre for Ecology and Hydrology (UKCEH), Wallingford, UK, <sup>3</sup>National Centre for Earth Observation (NCEO), Wallingford, UK

**Abstract** Understanding controls on Mesoscale Convective Systems (MCSs) is critical for predicting rainfall extremes across scales. Spatial variability of soil moisture (SM) presents such a control, with ~200 km dry patches in the Sahel observed to intensify mature MCSs. Here we test MCS sensitivity to spatial scales of surface heterogeneity using a framework of 78 Unified Model experiments initialized from scale-filtered SM. We demonstrate the control of SM heterogeneity on MCS populations, and the mechanistic chain via which spatial variability propagates through surface fluxes to convective boundary layer development and storm environments. When all sub-synoptic SM variability is homogenized, peak MCS counts drop by 23%, whereas maintaining small-scale variability maintains primary initiation rates, reducing the drop in MCS totals. In sensitivity experiments, boundary layer development prior to MCSs is similar to that over mesoscale dry SM anomalies, but driven by cloud-free slots of increased shortwave radiation. This reduces storm numbers and potential predictability.

Plain Language Summary Tropical rainfall is dominated by Mesoscale Convective Systems (MCSs), large, long-lived organized clusters of thunderstorms. Storm properties are determined in part by the balance of surface fluxes of heat and moisture. Over semi-arid land regions such as the African Sahel, these fluxes are controlled by soil moisture (SM) content. Observations show that the impact of SM on MCS processes then varies depending on the scale of spatial variability of the SM field. Here we assess the sensitivity of Sahelian MCSs to scales of SM variability by running 78 high-resolution atmospheric simulations in which only the early morning land surface is altered. In one experiment set we suppress all SM variability below ~1,000 km, yielding a homogeneous land-state, while another experiment reintroduces small-scale SM variability. Both experiments yield a significant reduction in MCS numbers, with the strongest effect in experiments with homogeneous SM. Warm planetary boundary layer conditions which support subsequent MCS activity are typically found over mesoscale dry SM anomalies. When SM is homogenized, high insolation plays an increasing role in creating the locally warm conditions favoring convection. This reduces storm numbers, and likely also predictability, since cloud-free areas are more diffuse and transient than SM patches.

### 1. Introduction

Mesoscale Convective Systems (MCSs), large organized convective storms which play a prominent role in tropical weather and climate, show significantly different characteristics over land versus oceans (e.g., Abbott et al., 2025). This high-level comparison highlights the striking fact that the balance of surface turbulent fluxes exerts a major influence on one of the primary sources of tropical rainfall. Deep convective organization and intensity is determined by atmospheric drivers such as moisture, Convective Available Potential Energy (CAPE) and wind shear, the local balance of which characterizes different MCS hotspots and explains their geographical occurrence across spatial scales (Laing & Fritsch, 2000; Schumacher & Rasmussen, 2020). The inherent orographic, biophysical and hydrological heterogeneity of the land-surface leads to spatial variability in latent and sensible heat flux partitioning, and thereby planetary boundary layer (PBL) development (Betts & Ball, 1995; Carson, 1973; Huang & Margulis, 2013), altering local balances of convective drivers.

Where soil moisture (SM) deficits strongly influence the surface flux partition of available energy there can be significant feedbacks on convective rainfall (Koster et al., 2004). In principle, a chain of local couplings to the atmospheric column can affect the initiation and development of convection (LoCo, Santanello et al., 2018), providing analytical understanding of when convective triggering may occur (Bhowmick & Parker, 2018; Findell

MAYBEE ET AL. 1 of 11 Supervision: John H. Marsham Visualization: Ben Maybee Writing – original draft: Ben Maybee Writing – review & editing: Ben Maybee, Cornelia Klein, Christopher M. Taylor, Helen Burns, John H. Marsham & Eltahir, 2003). However, observations suggest that non-local mechanisms dependent on the spatial variability of SM (SM heterogeneity henceforth) must be invoked to fully understand land–atmosphere interactions with precipitation, P (Guillod et al., 2015; Hsu et al., 2017).

This is especially the case for MCSs, which respond to SM heterogeneity at scales from tens to hundreds of kilometers through the generation of daytime mesoscale circulations (Taylor et al., 2007). In the Sahel region of West Africa, the likelihood of MCS initiation is doubled over ~30 km SM gradients due to enhanced local convergence (Taylor et al., 2011); the region's relatively uniform topography and absence of irrigation isolate this signal, but such controls on initiation are observed in other continents (Gaal & Kinter, 2021; Taylor, 2015; Teramura et al., 2019). At the synoptic scale, Barton et al. (2025) show that meridional SM gradients intensify mature MCSs by strengthening vertical wind shear in multiple semi-arid regions, including West Africa. Here regional SM strongly influences the midlevel African Easterly Jet (AEJ), an integral feature of the West African Monsoon (WAM) circulation (Cook, 1999; Talib et al., 2022).

The Sahel is characterized by a negative SM–P feedback (Taylor et al., 2013). In particular, mesoscale ( $\sim$ 200 km) dry SM anomalies are observed to intensify mature MCSs (Klein & Taylor, 2020). Filling the spectrum of spatial heterogeneity, such patches are found to build favorable conditions for intense convection through a combination of convergence, increased instability and wind shear. This feedback imbues the Sahelian land-surface with short-term predictive skill (Taylor et al., 2022), with mesoscale wet patches deposited by storm rainfall exerting multiday suppression of following events (Taylor et al., 2024) and causing severe wet-bulb temperature events (Chagnaud et al., 2025). MCS activity over the Sahel is intensifying under climate change (Taylor et al., 2017), with potentially fewer, more extreme storms in the future (Kendon et al., 2019). This could enhance SM heterogeneity at the mesoscale (e.g., Guilloteau et al., 2025; Hsu & Fueglistaler, 2025) and thereby likely further exacerbate future extremes.

Such feedbacks are poorly represented in coarse-gridded global climate simulations that must parameterize deep convection (Taylor et al., 2012). The sign of the SM-P feedback depends on the treatment of convection (Hohenegger et al., 2009), especially regarding the impact of heterogeneity (Taylor et al., 2013), while Lee and Hohenegger (2024) found a convection permitting (CP) global simulation weakens positive temporal SM-P correlations. Kilometer-scale CP models provide significantly improved representation of both land-surface features and MCS dynamics, realistically simulating the diurnal cycles of MCSs (Prein et al., 2015) and their responses to environmental drivers (Maybee et al., 2024). However, MCS populations in global CP models show other systematic biases (Feng et al., 2023, 2025), making process—analysis of MCS drivers, including land-atmosphere interactions, an integral component of model evaluation.

It is therefore important to interrogate the sensitivity of MCS populations to changes in SM heterogeneity across scales, since such heterogeneity is itself resolved in kilometer-scale models. We explore this question in the Sahel using two sets of CP sensitivity experiments comprising daily restarts from an evolving SM field with filtered variability at selected scales. Other studies tackle small-scale effects in other regions (Gaal et al., 2024; Paccini & Schiro, 2025), however our unique setup enables an isolation of mesoscale feedbacks on mature systems. We show that suppression of SM heterogeneity significantly diminishes MCS numbers, and elucidate the land-atmosphere interactions responsible.

#### 2. Scale Sensitivity Experiments

We utilize high-resolution CP model experiments run with the Met Office Unified Model (MetUM, Brown et al., 2012). All experiments feature a 1.5 km grid spacing; the RAL3.1 physics configuration (Bush et al., 2025) of default regional modeling settings and parameterizations of sub-grid processes; and the JULES land-surface scheme (Best et al., 2011).

A simulation spanning 25 July 2006–09 March 2006 was initialized at 00 UTC on 23 July 2006 using ERA5 atmospheric conditions (Hersbach et al., 2020) and (4 level) SM derived from a previous 10 years CP MetUM experiment (Stratton et al., 2018). Since our simulation used identical soil properties as this model, the SM profile was already spun-up and we analyzed all but the first 48 hr. The 1.5 km West Africa domain is nested within a 4 km simulation (Figure S1a in Supporting Information S1) that itself takes ERA5 boundary conditions every 6 hr. From the 1.5 km simulation we extract the 06 UTC atmospheric and land-surface state from 25 July 2006 to 01

MAYBEE ET AL. 2 of 11

19448007, 2025, 22, Downloaded from https://agupubs.onlinelibrary.wiley.com/doi/10.1029/2025GL118583 by UK Centre For Ecology & Hydrology, Wiley Online Library on [24/11/2025]. See the Terms

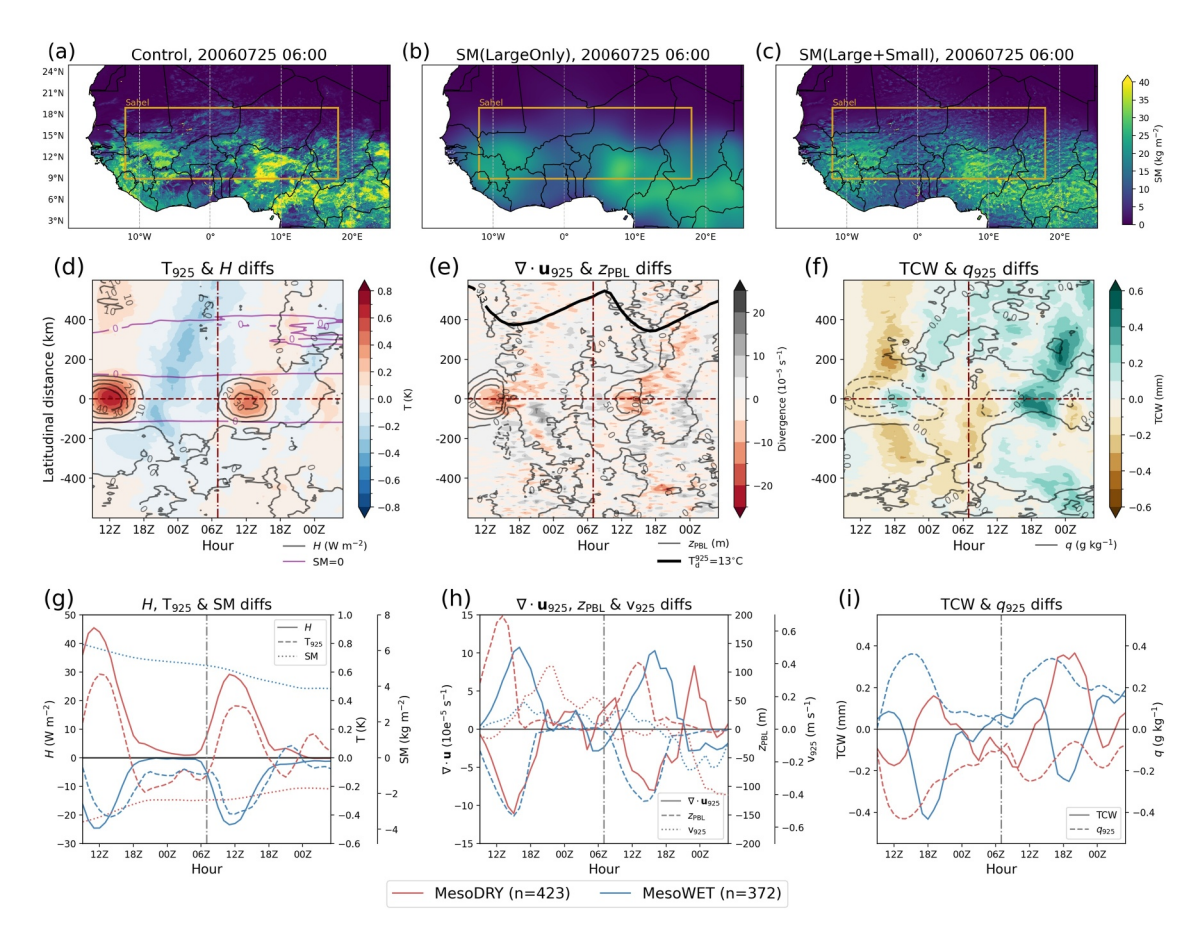


**Figure 1.** (a–c) Representative 06 UTC surface-layer soil moisture (SM) content for each simulation; boxes show Sahel domain. (d–f) Composite evolution about MesoDRY locations of difference between Control and SM(Large + Small) (d) sensible heat flux and 925 hPa temperature; (e) planetary boundary layer height and 925 hPa divergence; and (f) total column water and 925 hPa humidity. Control mean intertropical discontinuity (bold 925 hPa 13°C dewpoint contour) shown in panel (e). (g–i) Area-averaged evolution of same field differences about MesoDRY and MesoWET locations, also with (g) SM and (h) 925 hPa meridional wind. All averages taken over 150 km slices.

September 2006. These fields then provide the initial conditions for 39 groups of restarted 48 hr long runs where the only alteration made to the initial conditions is in the top (10 cm deep) SM layer.

#### 2.1. Control and SM(LargeOnly)

Our first target is to suppress all SM heterogeneity while maintaining large-scale patterns that feed-back on synoptic atmospheric features such as the AEJ (Cook, 1999). We apply a Gaussian filter with kernel radius of 600 km to the 06 UTC SM field—this suppresses all sub-synoptic scale variability while only marginally weakening the meridional gradient across our primary study region, the Sahel (Figures 1a and 1b; -12°-18°E, 9°-19°N).

We also reinitialize companion 48-hr Control runs, in which no changes are made to the 06 UTC land surface. All anomalies are calculated against Control means throughout. Comparing the time evolution of the simulations' respective power spectra (Figure S1b in Supporting Information S1) shows the expected suppression of variability in SM(LargeOnly) for scales below 1,000 km throughout the full experiment, but with a modest recovery in sub–200 km variability due to convective activity reintroducing SM features at these scales. Figure S2 in Supporting Information S1 shows the mean state of the WAM system remains very similar between SM(LargeOnly) and Control; any differences between the models can therefore be attributed to the impact of the land-surface on subsynoptic scale processes.

MAYBEE ET AL. 3 of 11

The SM(LargeOnly) experiments remove SM variability <1,000 km. In order to isolate the control of mesoscale SM variability on mature convection, we also run a SM(Large + Small) experiment where we reintroduce SM patchiness at scales <100 km, excluding only the mesoscale 100-500 km scale range. We quantify variability at a given spatial scale using a wavelet transform onto an isotropic Marr/Mexican-hat basis initialized across 40 scales starting from 4 km (see Wang and Lu (2010) and Klein et al. (2018)). To construct a 06 UTC SM field from which mesoscale variability is removed, we set the wavelet coefficients for scales above 100 km to zero and apply an inverse transform on the same basis. This field, which comprises a reconstruction of all small-scale (<100 km) variability, is then added to the Gaussian-smoothed field used to initialize SM(Large Only). The 39 resulting SM fields are used to initialize the second experiment set, SM(Large + Small).

The reinstatement of small spatial scales in SM(Large + Small) versus SM(LargeOnly) is clearly visible from Figure 1c, while intermediate scales are still missing versus Control. Analysis of power spectra confirms this (Figure S1c in Supporting Information S1), with variability suppressed versus Control at the mesoscale. Synoptic mean states are again comparable (Figure S2 in Supporting Information S1).

### 3. SM Derived Changes to PBL

Before considering MCSs, we first isolate mesoscale SM patches' impact on PBL development without reference to convection. To do so, we identify locations where mesoscale patches were removed by wavelet-transforming each D1 09 UTC (+3 hr) SM difference field between Control and SM(Large + Small), isolating regions where the resulting variance-normalized power spectrum is >2 (i.e.,  $\sim95\%$  significant). Sample locations are then power maxima for scales between 150 and 650 km, with the largest scale used where a region shows multiple maxima. Our sampling ensures we only consider locations where strong mesoscale SM anomalies were removed, resulting in 423 cases for dry (MesoDRY) and 372 cases for wet (MesoWET) anomalies.

MesoDRY control on PBL development over two diurnal cycles is shown by composite Hovmoellers (Figures 1d–1f, MesoWET counterparts Figure S3 in Supporting Information S1) of the difference between Control and SM(Large + Small) fields. Since the only change to our sensitivity experiments is the initial SM, such differences isolate the effect that SM anomalies in Control have on atmospheric fields. Centering on MesoDRY locations, that is, where there is a dry patch, we find a mesoscale region of strong sensible heat fluxes H. PBL temperatures T are thus elevated, and there is colocated, mesoscale growth of PBL height ( $z_{PBL}$ , Figure 1e). This generates low-level convergence ( $\nabla \cdot \mathbf{u}$ ) soon after midday, enhancing southerly meridional winds  $\nu$  (Figure 1h) while the intertropical discontinuity shifts southward.

Dry patches cause a mesoscale suppression of latent heat flux  $L_cE$  (not shown), reducing low-level moisture near the patch (Figure 1f, vertical sections Figure S4b in Supporting Information S1). There is a complementary relative moistening of air above  $z_{\rm PBL}$ , caused by increased entrainment of dry air into the PBL under elevated H. Overall, total column water (TCW) increases from 14 UTC onwards (Figures 1f and 1i). This is driven by the mesoscale low-level convergence, which generates net ascent and from 15 UTC-onwards, column moisture convergence (Figure S4g in Supporting Information S1), with the feedback further enhanced on day 2 (D2). Moreover, the dynamical changes enhance the local monsoon flow: nocturnal north-eastwards propagating bands of enhanced TCW (Figure 1f), reduced temperatures (Figure 1d), increased southerly winds (Figure 1h) and meridional moisture flux (Figure S4g in Supporting Information S1) indicate a strengthened WAM flow, peaking overnight (Parker et al., 2005).

Figures 1g-1i show MesoDRY/WET variables averaged across a 150 km box centered on identified patches. As expected, MesoWET locations show an opposite effect to MesoDRY, with a H deficit in Control versus SM (Large + Small) and  $L_cE$  instead increased, enhancing low-level moisture favorable for convection. However, absolute temperatures are reduced and  $z_{PBL}$  is lowered, strengthening divergence above the wet patch and yielding no monsoon enhancement. There is instead strengthened moisture divergence relative to MesoDRY (Figure S4h in Supporting Information S1), leading to decreased TCW from mid-afternoon onwards above the wet patch, above which we also find net subsidence. Indirect feedbacks of H on column moisture, mediated by dynamical changes to the WAM, are again stronger than direct feedbacks from surface evaporation, yielding enhanced TCW over dry SM patches and suppressed TCW over wet patches.

MAYBEE ET AL. 4 of 11

19448007, 2025, 22, Downloaded from https://agupubs.onlinelibrary.wiley.com/doi/10.1029/2025GL118583 by UK Centre For Ecology & Hydrology, Wiley Online Library on [24/11/2025]. See the Term

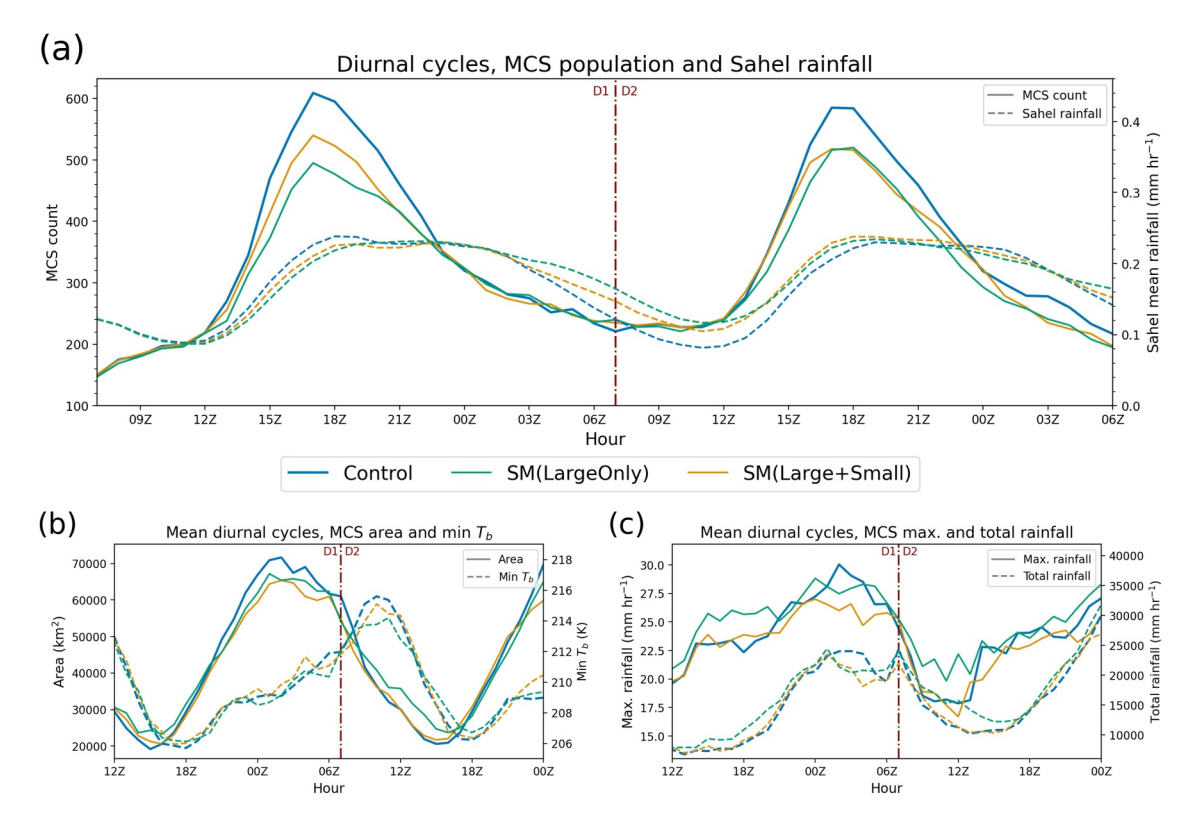


Figure 2. (a) Hourly total counts of tracked Sahel Mesoscale Convective System (MCS) snapshots (solid lines) and regional mean rainfall (dashed) across all 39 members of each simulation. (b) Mean MCS snapshot areas (solid) and minimum  $T_b$  (dashed) between 12 UTC D1 and 00 UTC D2. (c) Mean hourly MCS maximum (solid) and total (dashed) rainfall rates over same period.

In summary, mesoscale PBL deepening driven by enhanced *H* from underlying dry SM anomalies causes enhanced convergence and localized net ascent. In the Sahel, these dynamical feedbacks over dry soils enhance the monsoon flow and increase column moisture.

#### 4. SM-Driven Changes to MCSs

We now take a convection-centered perspective, focusing on mature storms. To identify MCSs we apply the simpleTrack algorithm (Stein et al., 2014), adopted and described in Maybee et al. (2025), applied to brightness temperatures ( $T_b$ ) calculated from total outgoing longwave radiation. Storms are tracked over the model domain and comprise snapshots where  $T_b < 241\,\mathrm{K}$  over a minimum area of 1,000 km², with candidate MCSs reaching a lifetime maximum area of at least 5,000 km² and minimum  $T_b < 223\,\mathrm{K}$ . For these tracks, rainfall volumes and extremes are calculated (from 0.1° regridded precipitation), with MCSs required to reach a maximum rainfall rate above 1 mm hr $^{-1}$  during the storm's lifetime.

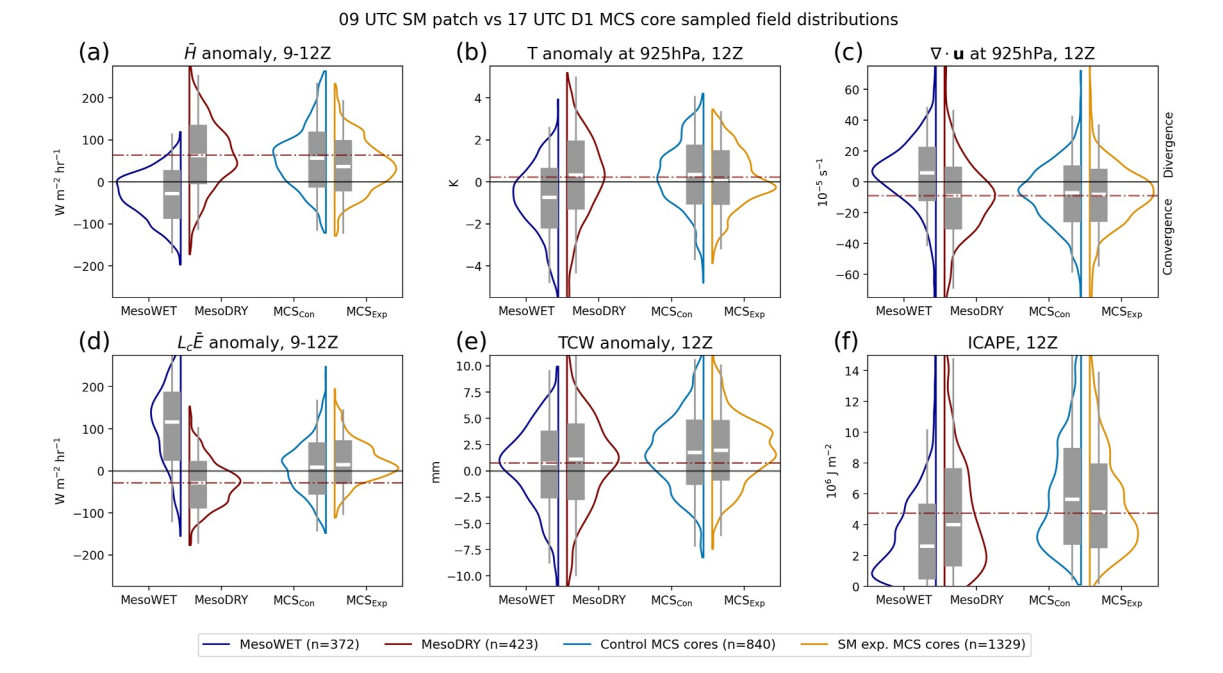
#### 4.1. Storm Characteristics

Figure 2a shows the combined diurnal cycles of the Sahelian MCS population across each set of simulations. All show identical phasings, with a 17 UTC peak in activity following primary initiation. However, amplitudes are significantly altered in the experiments: in SM(LargeOnly) the D1 peak storm count is 23% lower than in Control. On D2 in SM(LargeOnly) the population begins to recover, at 4% higher than D1 and 13% lower than the D2 Control peak. In SM(Large + Small), the drop in storm numbers is smaller than SM(LargeOnly), with the peak 13% lower than Control, but this does not recover into D2. We find no change in storm speeds and lifetimes in either experiment (not shown).

In both experiments, afternoon D1 mean Sahel rainfall and MCS activity is reduced, with regional totals and storm numbers equivalent to Control overnight. Concurrently, MCSs grow larger in Control than in the experiments (Figure 2b), but with comparable convective intensities as measured by cloud temperatures and storm rainfall

MAYBEE ET AL. 5 of 11

19448007, 2025, 22, Downloaded from https://agupubs.onlinelibrary.wiley.com/doi/10.1029/2025GL118583 by UK Centre For Ecology & Hydrology, Wiley Online Library on [2411/2025]. See



**Figure 3.** Violin and box plots of 1° mean (a) sensible heat flux and (b) 925 hPa temperature anomalies; (c) 925 hPa divergence; (d) latent heat flux and (e) total column water anomalies; and (f) integrated Convective Available Potential Energy. Distributions centered on D1 09 UTC MesoDRY/WET and 17 UTC Mesoscale Convective System (MCS) core locations, with sensitivity experiment MCS (MCS<sub>Exp</sub>) conditions aggregated from both experiments. All 12 UTC fields unless stated otherwise, legend specifies sample sizes. Soil moisture patches sampled in Control, horizontal red lines show MesoDRY means.

(Figures 2b and 2c, Figure S5a in Supporting Information S1). Fewer primary initiations in SM(LargeOnly) reduces the number of small systems (Figures S5b and S5c in Supporting Information S1), artificially inflating daytime mean MCS areas and rainfall. From 03 to 18 UTC D2 however, regional rainfall totals are lower in Control. This now reflects a relative intensification of convective activity in SM(LargeOnly): there are comparable MCS numbers (Figure 2a), of all sizes (Figure S5c in Supporting Information S1), but with larger, colder anvils (Figure 2b) and stronger rainfall (Figure 2c), coincident with higher mean regional rainfall and cloud cover (Figure S2c in Supporting Information S1). Relative recovery in Control then comes during the second afternoon.

We thus conclude that in the Sahel, SM heterogeneity exerts a significant positive feedback on afternoon MCS populations which is maintained through the diurnal peak and into the night. Storms that persist until the early morning of the next day, however, are relatively weakened.

#### 4.2. Mechanisms

To understand the land–atmosphere interactions which cause these impacts on regional MCSs, we examine land and atmospheric conditions prior to convective cores in mature MCSs at the diurnal peak (17 UTC) of convection. We define mature MCSs as  $T_b < 241 \, \mathrm{K}$  contiguous cloud covering an area  $> 15,000 \, \mathrm{km}^2$ , within which cores are identified as multi-pixel regions where the 500 hPa updraft velocity is greater than the 99.5th percentile of instorm values. We exclude cores located over orography above 450 m; where there was an MCS anvil covering the same location at 15 UTC; and where the enveloping MCS initiated less than 150 km away (Klein & Taylor, 2020). This avoids situations where local pre-core conditions have already been disturbed by the same MCS.

We compare distributions of D1 12 UTC pre-core environmental fields (Figure 3) between Control (MCS $_{Con}$ ) and the aggregated sensitivity experiments (MCS $_{Exp}$ ). Alongside, we show conditions developed by mesoscale SM patches by sampling Control fields at MesoDRY and MesoWET locations, hereby evaluating which distributions resemble pre-MCS conditions. Consistent with observations (Klein & Taylor, 2020), MCS $_{Con}$  cores are associated with pre-convective positive H and low-level temperature anomalies, comparable distributions of which are found over MesoDRY but not MesoWET locations (Figures 3a and 3b). Similar, but weaker, conditions are still evident for experiment cores despite the absence of mesoscale SM anomalies. This suggests the importance of an alternative mechanism establishing these environments in the sensitivity experiments. Meanwhile the low-level

MAYBEE ET AL. 6 of 11

convergence generated by MesoDRY SM perturbations resembles MCS distributions (Figure 3c), indicating they provide favorable environmental conditions for mature MCSs.

Latent fluxes are not a key influence on mature MCSs even in sensitivity experiments (Figure 3d), with high  $L_cE$  anomalies about MesoWET patches manifestly not favored by storm cores. However, cores remain located at positive low-level humidity (Figure S6a in Supporting Information S1) and TCW (Figure 3e) anomalies, emphasizing the background monsoon flow's role in generating favorable thermodynamic environments. As anticipated from Section 3, distributions of TCW about MesoDRY patches are therefore closer to those for MCSs than MesoWET, despite stronger low-level moisture anomalies about the latter.

Analogously to TCW, we can measure total column instability through integrated CAPE,

$$ICAPE = \frac{1}{g} \int dp \, CAPE(p), \tag{1}$$

where CAPE(p) > 0. Using soundings calculated from 1° mean profiles, we find the median ICAPE value is ~50% higher at MesoDRY locations than MesoWET, reflecting a distribution closer to that for MCS environments (Figure 3f). Near-surface parcel CAPE values about MesoWET are higher (Figure S6c in Supporting Information S1), but overall ICAPE better reflects the thermodynamic state across the full PBL (Alfaro & Khairoutdinov, 2015), the lifting of which has been proposed as a dynamical control on MCS convection (Alfaro, 2017). We find significantly higher thermodynamic instability prior to MCS cores than that originating from SM patches alone, indicating that favorable conditioning of the convective environment stems from the superposition of multiple mechanisms. Crucially though, such conditioning represents an enhancement of conditions about MesoDRY locations. Mesoscale wet patches meanwhile act as an inhibitor for mature MCSs, by suppressing favorable convective environments.

As noted previously, we continue to find mature MCSs in the experiments following positive H anomalies (Figure 3a). Why then are the storm populations so different? Examining the sampled environments' spatial structure (Figures 4a–4c) shows that H anomalies prior to  $MCS_{Exp}$  cores are driven by >200 km peaks in surface net shortwave radiation (SW<sub>sfc</sub>), rather than dry soil patches. There are no co-located peaks in  $L_cE$ .

The importance of insolation in driving H is confirmed by Hovmoellers (Figures 4d–4i) in advance of D2 MCS core occurrence. The SM(Large + Small) experiment (conditions closest to Control) shows a positive morning SW $_{\rm sfc}^{\rm net}$  anomaly (Figure 4g) spanning ~400 km and located in a region of reduced cloud cover. Similar behavior occurs on both days and in SM(LargeOnly) (Figure S7 in Supporting Information S1). Mesoscale shortwave variability is higher than in Control (Figure S1c in Supporting Information S1), which shows weaker and smaller pre-storm anomalies (Figure 4d), while cloud cover is increased. In all cases, SW $_{\rm sfc}^{\rm net}$  plummets after 14 UTC as MCS anvils develop and advance ahead of the convective cores.

Mesoscale positive PBL temperature and height anomalies are apparent before midday at all later core locations. These stem from the co-located *H* anomaly, and generate convergence prior to storms (Figure 1e). The primary difference in core-relative environments is low-level moisture and thermodynamic instability (Figures 4f and 4i), both of which increase prior to core occurrence. In agreement with observations (Klein & Taylor, 2020), southerly flow is responsible for this build-up: for evening MCSs, monsoon flow the night before is the primary source of column moisture, which during the day reinforces PBL development from surface *H* anomalies to provide an optimal convective environment. This mechanism is found in all simulations.

The primary role of dry mesoscale SM anomalies is thus to instigate the mechanism explored in Section 3 by causing *H* anomalies. When suppressed, this feedback can be driven by insolation from cloud-free slots. However, such patches are necessarily more diffuse and ephemeral than SM counterparts, reducing opportunities for the chain of PBL development to build conditions favorable for mature storms. This will reduce the MCS population, especially when combined with suppression of storm initiation from small-scale SM features (Figure 2a). The absence of mesoscale SM variability also removes wet patches. MCSs which do establish in the experiments therefore also lose an inhibitor, instead benefiting from continued nocturnal monsoon flows and relatively uniform high low-level humidity. Their population therefore comprises fewer storms, but of comparable intensity to Control (Figures 2b and 2c). Early morning relative intensification may then be due to modified

MAYBEE ET AL. 7 of 11

19448007, 2025, 22, Downloaded from https://agupubs.onlinelibrary.wiley.com/doi/10.1029/2025GL118583 by UK Centre For Ecology & Hydrology, Wiley Online Library on [24/11/2025]. See the Terms

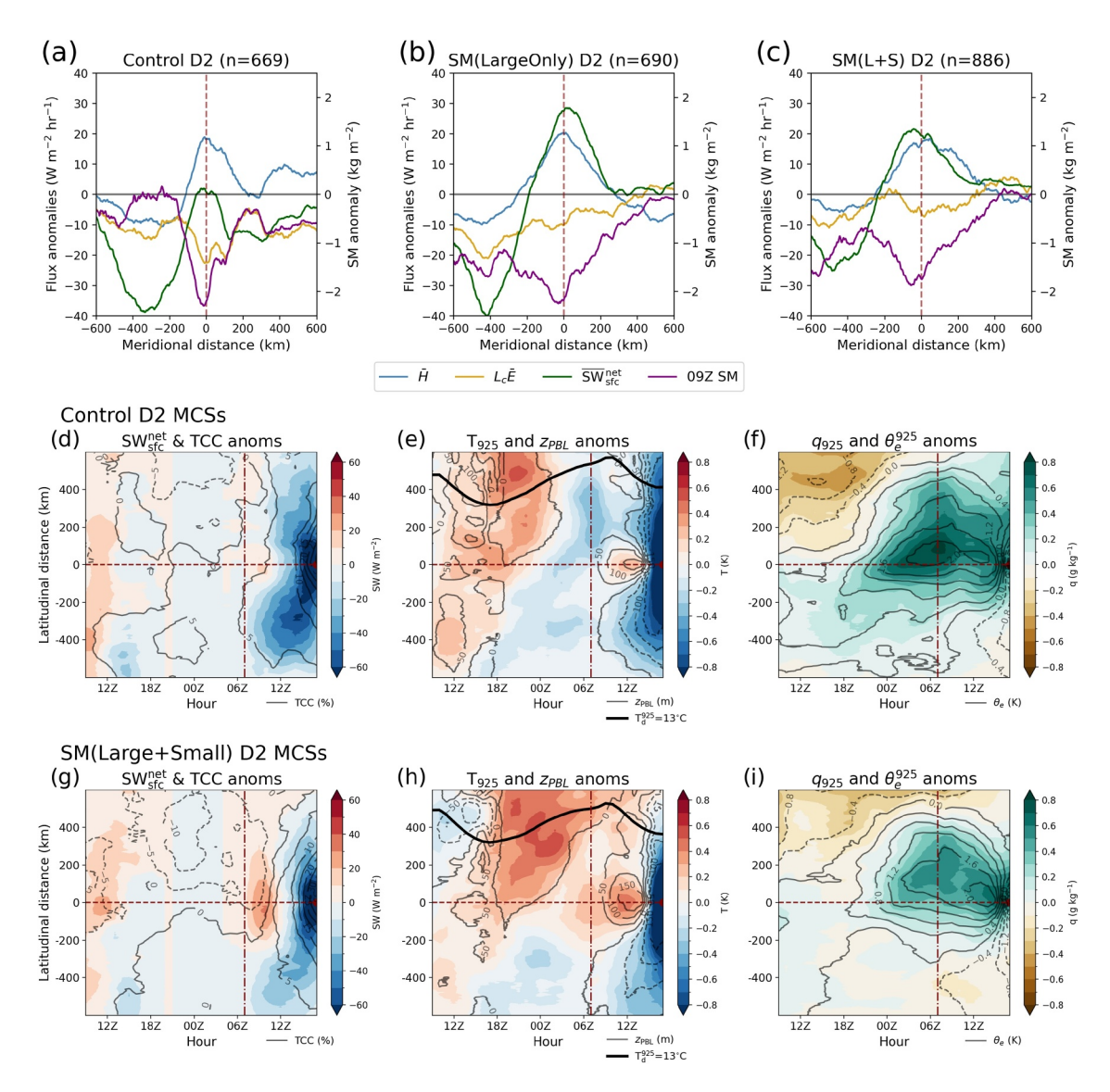


**Figure 4.** (a–c) Zonal sections, for each simulation, of composite mean 09–12 UTC flux anomalies at D2 locations of 17 UTC Sahel Mesoscale Convective System cores; titles specify sample sizes. (d–f) Composite Hovmoellers of evolution prior to Control D2 core locations of anomalous (d) shortwave radiation and total cloud cover; (e) planetary boundary layer height and 925 hPa temperature; and (f) 925 hPa humidity and equivalent potential temperature ( $\theta_e$ ). (g–i) Repeated for SM(Large + Small) D2. 150 km longitudinal slices used throughout; vertical lines denote start of D2.

land-surface interactions with cold pools (Drager et al., 2020; Gentine et al., 2016), which Sahelian MCS populations are most sensitive to around dawn (Maybee et al., 2025).

#### 5. Conclusions

This study has investigated the sensitivity of MCSs to scales of SM heterogeneity, testing feedbacks observed over the Sahel (Klein & Taylor, 2020; Taylor et al., 2007) in MetUM simulations initialized from modified 06 UTC SM fields. No other changes were made. In SM(LargeOnly) experiments where all sub-synoptic spatial SM variability was homogenized, we find a 23% decrease in MCS numbers at the Day 1 diurnal peak of convection versus Control simulations. This is a result of suppressing mesoscale dry patches (MesoDRY), which provide favorable dynamic and thermodynamic conditions for mature storms. For SM(Large + Small) experiments where only mesoscale SM variability is suppressed, the decline in storm population is smaller (–13%) due to higher rates of primary initiation than over homogenous SM, consistent with the role of small-scale SM gradients in enhancing MCS initiation (Taylor et al., 2011). A full SM spectrum also contains mesoscale wet

MAYBEE ET AL. 8 of 11

/10.1029/2025GL118583 by UK Centre For Ecology & Hydrology, Wiley Online Library on [24/11/2025]. See the Term

Acknowledgments

The research presented here was conducted

funding from the NERC fellowship project

Doug Parker, Emma Barton, Brian Mapes,

and Yutong Lu for related discussions and

comments, and two anonymous referees

whose reviews have improved our paper.

All simulations were run on ARCHER2,

the UK National Supercomputing Service

(Beckett et al., 2024), with data analysis

conducted on JASMIN, the UK national

collaborative data analysis facility.

within the NERC funded LMCS project

(NE/W001888/1). C. K. acknowledges

COCOON (NE/X017419/1). We thank

patches (MesoWET), which inhibit storms by suppressing favorable convective environments. These are also suppressed in both experiments, leading to comparable peak MCS intensities to Control despite declines in storm numbers.

Our results demonstrate the significant control SM variability can exert on MCS populations. As context, a similar experiment targeting the region's storms' sensitivity to cold pools (Maybee et al., 2025) demonstrated only a 4% reduction in peak MCS population, but stronger changes to convective intensity. In the Sahel, SM heterogeneity therefore plays a stronger role in supporting MCS populations than cold pools, with the interplay of these sensitivities demanding future investigation. Significant influences of land–atmosphere interactions on MCS dynamics occur globally (Barton et al., 2025): our study highlights the relative magnitude of these effects.

In both experiments we find PBL development before MCS cores similar to that in Control prior to MCSs, and following dry SM patches. However, the crucial morning *H* anomaly is instead driven by insolation over cloud-free slots. This has important implications for predictability. The Sahelian land-surface has a 2 weeks memory of MCS passage, with a lagged effect on rainfall up to 8 days (Taylor et al., 2024), and can be utilized operationally for nowcasting (Taylor et al., 2022). Feedbacks stemming from insolation lose this multi-scale predictability, thereby reducing the predictability of MCS behavior. The land–atmosphere interactions in the Sahel are thus advantageous for local forecasting of convection versus regions with homogenous SM, and show the benefit of identifying and utilizing these mechanisms for other regions with mesoscale surface heterogeneity.

#### **Conflict of Interest**

The authors declare no conflicts of interest relevant to this study.

#### **Data Availability Statement**

Code and data underpinning this research are available publicly at Maybee (2025).

#### References

Abbott, T. H., Jeevanjee, N., Cheng, K.-Y., Zhou, L., & Harris, L. (2025). The land-ocean contrast in deep convective intensity in a global storm-resolving model. *Journal of Advances in Modeling Earth Systems*, 17(5), e2024MS004467. https://doi.org/10.1029/2024MS004467

Alfaro, D. A. (2017). Low-tropospheric shear in the structure of squall lines: Impacts on latent heating under layer-lifting ascent. *Journal of the Atmospheric Sciences*, 74(1), 229–248. https://doi.org/10.1175/JAS-D-16-0168.1

Alfaro, D. A., & Khairoutdinov, M. (2015). Thermodynamic constraints on the morphology of simulated midlatitude squall lines. *Journal of the Atmospheric Sciences*, 72(8), 3116–3137, https://doi.org/10.1175/JAS-D-14-0295.1

Barton, E. J., Klein, C., Taylor, C. M., Marsham, J. H., Parker, D. J., Maybee, B., et al. (2025). Storm intensification driven by soil moisture gradients in global hotspot regions. *Nature Geoscience*, 18(4), 330–336. https://doi.org/10.1038/s41561-025-01666-8

Beckett, G., Beech-Brandt, J., Leach, K., Payne, Z., Simpson, A., Smith, L., et al. (2024). ARCHER2 service description. Zenodo. https://doi.org/10.5281/zenodo.14507040

Best, M. J., Pryor, M., Clark, D. B., Rooney, G. G., Essery, R., Ménard, C. B., et al. (2011). The Joint UK Land Environment Simulator (JULES), model description—Part 1: Energy and water fluxes. *Geoscientific Model Development*, 4(3), 677–699. https://doi.org/10.5194/gmd-4-677-2011

Betts, A. K., & Ball, J. (1995). The FIFE surface diurnal cycle climate. *Journal of Geophysical Research*, 100(D12), 25679–25693. https://doi.org/10.1029/94JD03121

Bhowmick, M., & Parker, D. J. (2018). Analytical solution to a thermodynamic model for the sensitivity of afternoon deep convective initiation to the surface Bowen ratio. *Quarterly Journal of the Royal Meteorological Society*, 144(716), 2216–2229. https://doi.org/10.1002/qj.3340

Brown, A., Milton, S., Cullen, M., Golding, B., Mitchell, J., & Shelly, A. (2012). Unified modeling and prediction of weather and climate: A 25–year journey. Bulletin of the American Meteorological Society, 93(12), 1865–1877. https://doi.org/10.1175/BAMS-D-12-00018.1

Bush, M., Flack, D. L. A., Lewis, H. W., Bohnenstengel, S. I., Short, C. J., Franklin, C., et al. (2025). The third Met Office Unified Model–JULES Regional Atmosphere and Land configuration, RAL3. *Geoscientific Model Development*, 18(12), 3819–3855. https://doi.org/10.5194/gmd-18-3819-2005

Carson, D. J. (1973). The development of a dry inversion-capped convectively unstable boundary layer. Quarterly Journal of the Royal Mete-orological Society, 99(421), 450–467. https://doi.org/10.1002/qj.49709942105

Chagnaud, G., Taylor, C. M., Jackson, L. S., Birch, C. E., Marsham, J. H., & Klein, C. (2025). Wet-bulb temperature extremes locally amplified by wet soils. Geophysical Research Letters, 52(8), e2024GL112467. https://doi.org/10.1029/2024GL112467

Cook, K. H. (1999). Generation of the African easterly jet and its role in determining West African precipitation. *Journal of Climate*, 12(5), 1165–1184. https://doi.org/10.1175/1520-0442(1999)012(1165:GOTAEJ)2.0.CO;2

Drager, A. J., Grant, L. D., & van den Heever, S. C. (2020). Cold pool responses to changes in soil moisture. *Journal of Advances in Modeling Earth Systems*, 12(8), e2019MS001922. https://doi.org/10.1029/2019MS001922

Feng, Z., Leung, L. R., Hardin, J., Terai, C. R., Song, F., & Caldwell, P. (2023). Mesoscale convective systems in DYAMOND global convection—permitting simulations. *Geophysical Research Letters*, 50(4), e2022GL102603. https://doi.org/10.1029/2022GL102603

Feng, Z., Prein, A. F., Kukulies, J., Fiolleau, T., Jones, W. K., Maybee, B., et al. (2025). Mesoscale convective systems tracking method intercomparison (MCSMIP): Application to DYAMOND global km-scale simulations. *Journal of Geophysical Research: Atmospheres*, 130(8), e2024JD042204. https://doi.org/10.1029/2024JD042204

130(8), e2024JD042204. https://doi.org/10.1029/2024JD042204

MAYBEE ET AL. 9 of 11

- Findell, K. L., & Eltahir, E. A. B. (2003). Atmospheric controls on soil moisture–boundary layer interactions. Part I: Framework development. Journal of Hydrometeorology, 4, 552–569. https://doi.org/10.1175/1525-7541(2003)004(0552:ACOSML)2.0.CO;2
- Gaal, R., & Kinter, J. L. (2021). Soil moisture influence on the incidence of summer mesoscale convective systems in the US Great Plains. Monthly Weather Review, 149(12), 3981–3994. https://doi.org/10.1175/MWR-D-21-0140.1
- Gaal, R., Kinter, J. L., Dirmeyer, P. A., & Singh, B. (2024). Identifying the mechanism of interaction between soil moisture state and summertime MCS initiations in weakly forced synoptic environments using convective-permitting simulations. *Journal of Geophysical Research: Atmospheres*, 129(23), e2024JD040855, https://doi.org/10.1029/2024JD040855
- Gentine, P., Garelli, A., Park, S.-B., Nie, J., Torri, G., & Kuang, Z. (2016). Role of surface heat fluxes underneath cold pools. *Geophysical Research Letters*, 43(2), 874–883. https://doi.org/10.1002/2015GL067262
- Guillod, B. P., Orlowsky, B., Miralles, D. G., Teuling, A. J., & Seneviratne, S. I. (2015). Reconciling spatial and temporal soil moisture effects on afternoon rainfall. *Nature Communications*, 6(1), 6443. https://doi.org/10.1038/ncomms7443
- Guilloteau, C., Chen, X., Leung, L. R., & Foufoula-Georgiou, E. (2025). Amplified mesoscale and submesoscale variability and increased concentration of precipitation under global warming over Western North America. *Journal of Climate*, 38(11), 2525–2542. https://doi.org/10.1175/JCLI-D-24-0343.1
- Hersbach, H., Bell, B., Berrisford, P., Hirahara, S., Horányi, A., Muñoz-Sabater, J., et al. (2020). The ERA5 global reanalysis. *Quarterly Journal of the Royal Meteorological Society*, 146(730), 1999–2049. https://doi.org/10.1002/qj.3803
- Hohenegger, C., Brockhaus, P., Bretherton, C. S., & Schär, C. (2009). The soil moisture–precipitation feedback in simulations with explicit and parameterized convection. *Journal of Climate*, 22(19), 5003–5020. https://doi.org/10.1175/2009JCL12604.1
- Hsu, H., & Fueglistaler, S. (2025). Robust projections of changing precipitation evenness in a warming climate. Geophysical Research Letters, 52(9), e2025GL114953. https://doi.org/10.1029/2025GL114953
- Hsu, H., Lo, M.-H., Guillod, B. P., Miralles, D. G., & Kumar, S. (2017). Relation between precipitation location and antecedent/subsequent soil moisture spatial patterns. *Journal of Geophysical Research: Atmospheres*, 122(12), 6319–6328. https://doi.org/10.1002/2016JD026042
- Huang, H.-Y., & Margulis, S. A. (2013). Impact of soil moisture heterogeneity length scale and gradients on daytime coupled land-cloudy boundary layer interactions. *Hydrological Processes*, 27(14), 1988–2003. https://doi.org/10.1002/hyp.9351
- Kendon, E. J., Stratton, R. A., Tucker, S., Marsham, J. H., Berthou, S., Rowell, D. P., & Senior, C. A. (2019). Enhanced future changes in wet and dry extremes over Africa at convection-permitting scale. *Nature Communications*, 10(1), 1794. https://doi.org/10.1038/s41467-019-09776-9
- Klein, C., Belušić, D., & Taylor, C. M. (2018). Wavelet scale analysis of Mesoscale Convective Systems for detecting deep convection from infrared imagery. *Journal of Geophysical Research: Atmospheres*, 123(6), 3035–3050. https://doi.org/10.1002/2017jD027432
- Klein, C., & Taylor, C. M. (2020). Dry soils can intensify Mesoscale Convective Systems. Proceedings of the National Academy of Sciences of the United States of America, 117(35), 21132–21137. https://doi.org/10.1073/pnas.2007998117
- Koster, R. D., Dirneyer, P. A., Guo, Z., Bonan, G., Chan, E., Cox, P., et al. (2004). Regions of strong coupling between soil moisture and
- precipitation. Science, 305(5687), 1138–1140. https://doi.org/10.1126/science.1100217

  Laing, A. G., & Fritsch, J. M. (2000). The large-scale environments of the global populations of mesoscale convective complexes. Monthly
- Weather Review, 128(8), 2756–2776. https://doi.org/10.1175/1520-0493(2000)128\(2756:TLSEOT\()2.0.CO;2
  Lee, J., & Hohenegger, C. (2024). Weaker land-atmosphere coupling in global storm-resolving simulation. Proceedings of the National Academy
- of Sciences of the United States of America, 121(12), e2314265121. https://doi.org/10.1073/pnas.2314265121
- $Maybee, B.~(2025).~\textit{BMaybee/MCS\_SM\_scales}.~Zenodo.~https://doi.org/10.5281/zenodo.16612936$
- Maybee, B., Bassford, J., Marsham, J. H., Lewis, H., Field, P., Klein, C., & Parker, D. J. (2025). How sensitive are Sahelian Mesoscale Convective Systems to cold pool suppression? *Quarterly Journal of the Royal Meteorological Society*, e5032, e5032. https://doi.org/10.1002/qj.5032
- Maybee, B., Marsham, J. H., Klein, C., Parker, D. J., Barton, E. J., Taylor, C. M., et al. (2024). Wind shear effects in convection-permitting models influence MCS rainfall and forcing of tropical circulation. Geophysical Research Letters, 51(17), e2024GL110119. https://doi.org/10.1029/2024GL110119
- Paccini, L., & Schiro, K. A. (2025). Influence of soil moisture on the development of organized convective systems in South America. *Journal of Geophysical Research: Atmospheres*, 130(9), e2024JD042108. https://doi.org/10.1029/2024JD042108
- Parker, D. J., Burton, R. R., Diongue-Niang, A., Ellis, R. J., Felton, M., Taylor, C. M., et al. (2005). The diurnal cycle of the West African monsoon circulation. *Quarterly Journal of the Royal Meteorological Society*, 131(611), 2839–2860. https://doi.org/10.1256/qj.04.52
- Prein, A. F., Langhans, W., Fosser, G., Ferrone, A., Ban, N., Goergen, K., et al. (2015). A review on regional convection-permitting climate modeling: Demonstrations, prospects, and challenges. Reviews of Geophysics, 53(2), 323–361. https://doi.org/10.1002/2014RG000475
- Santanello, J. A., Dirmeyer, P. A., Ferguson, C. R., Findell, K. L., Tawfik, A. B., Berg, A., et al. (2018). Land–atmosphere interactions: The LoCo perspective. *Bulletin of the American Meteorological Society*, 99(6), 1253–1272. https://doi.org/10.1175/BAMS-D-17-0001.1
- Schumacher, R. S., & Rasmussen, K. L. (2020). The formation, character and changing nature of mesoscale convective systems. *Nature Reviews Earth & Environment*, 1(6), 300–314. https://doi.org/10.1038/s43017-020-0057-7
- Stein, T. H., Hogan, R. J., Hanley, K. E., Nicol, J. C., Lean, H. W., Plant, R. S., et al. (2014). The three-dimensional morphology of simulated and observed convective storms over southern England. *Monthly Weather Review*, 142(9), 3264–3283. https://doi.org/10.1175/MWR-D-13-00372.1
- Stratton, R. A., Senior, C. A., Vosper, S. B., Folwell, S. S., Boutle, I. A., Earnshaw, P. D., et al. (2018). A Pan–African convection-permitting regional climate simulation with the Met Office Unified Model: CP4-Africa. *Journal of Climate*, 31(9), 3485–3508. https://doi.org/10.1175/JCLI-D-17-0503.1
- Talib, J., Taylor, C. M., Klein, C., Harris, B. L., Anderson, S. R., & Semeena, V. S. (2022). The sensitivity of the West African monsoon circulation to intraseasonal soil moisture feedbacks. *Quarterly Journal of the Royal Meteorological Society*, 148(745), 1709–1730. https://doi.org/10.1002/qj.4274
- Taylor, C. M. (2015). Detecting soil moisture impacts on convective initiation in Europe. *Geophysical Research Letters*, 42(11), 4631–4638. https://doi.org/10.1002/2015GL064030
- Taylor, C. M., Belušić, D., Guichard, F., Parker, D. J., Vischel, T., Bock, O., et al. (2017). Frequency of extreme Sahelian storms tripled since 1982 in satellite observations. *Nature*, 544(7651), 475–478. https://doi.org/10.1038/nature22069
- Taylor, C. M., Birch, C. E., Parker, D. J., Dixon, N., Guichard, F., Nikulin, G., & Lister, G. M. (2013). Modeling soil moisture-precipitation feedback in the Sahel: Importance of spatial scale versus convective parameterization. *Geophysical Research Letters*, 40(23), 6213–6218. https://doi.org/10.1002/2013GL058511
- Taylor, C. M., de Jeu, R. A., Guichard, F., Harris, P. P., & Dorigo, W. A. (2012). Afternoon rain more likely over drier soils. *Nature*, 489(7416), 423–426. https://doi.org/10.1038/nature11377
- Taylor, C. M., Gounou, A., Guichard, F., Harris, P. P., Ellis, R. J., Couvreux, F., & De Kauwe, M. (2011). Frequency of Sahelian storm initiation enhanced over mesoscale soil-moisture patterns. *Nature Geoscience*, 4(7), 430–433. https://doi.org/10.1038/ngeo1173

MAYBEE ET AL. 10 of 11

## **Geophysical Research Letters**

- 10.1029/2025GL118583
- Taylor, C. M., Klein, C., Dione, C., Parker, D. J., Marsham, J., Diop, C. A., et al. (2022). Nowcasting tracks of severe convective storms in West Africa from observations of land surface state. *Environmental Research Letters*, 17(3), 034016. https://doi.org/10.1088/1748-9326/ac536d
- Taylor, C. M., Klein, C., & Harris, B. L. (2024). Multiday soil moisture persistence and atmospheric predictability resulting from Sahelian Mesoscale Convective Systems. *Geophysical Research Letters*, 51(20), e2024GL109709. https://doi.org/10.1029/2024GL109709
- Taylor, C. M., Parker, D. J., & Harris, P. P. (2007). An observational case study of mesoscale atmospheric circulations induced by soil moisture. Geophysical Research Letters, 34(15), L15801. https://doi.org/10.1029/2007GL030572
- Teramura, H., Sato, T., & Tamura, K. (2019). Observed evidence of enhanced probability of Mesoscale Convective System initiations due to land surface heterogeneity in semiarid east Asia. Scientific Online Letters on the Atmosphere, 15, 143–148. https://doi.org/10.2151/sola.2019-026
- Wang, N., & Lu, C. (2010). Two-dimensional continuous wavelet analysis and its application to meteorological data. *Journal of Atmospheric and Oceanic Technology*, 27(4), 652–666. https://doi.org/10.1175/2009JTECHA1338.1

MAYBEE ET AL. 11 of 11